Numerical study on pile group efficiency for piles embedded in cohesive and cohesionless soils

Ignatius Tommy Pratama[1], *Budijanto* Widjaja[1*], and *Kelvin Agustinus* Budianto[2]

[1]Department of Civil Engineering, Universitas Katolik Parahyangan, Jl. Ciumbuleuit No. 94, Bandung, 40141
[2]Undergraduate Program in Department of Civil Engineering, Universitas Katolik Parahyangan, Jl. Ciumbuleuit No. 94, Bandung, 40141

Abstract. This paper aims to study the efficiency of pile groups with various numbers of piles and pile spacing. Axial loading tests on pile groups and also single piles were simulated using a three-dimensional finite element program to obtain the load-settlement curve and the ultimate bearing capacity of the piles which was later used to estimate the pile group efficiency. In this study, the piles were embedded in cohesive and cohesionless soils. The stress-strain responses of the soils and the concrete pile and pile cap were simulated using the Mohr-Coulomb and the linear elastic models, respectively. The numerical-based pile group efficiencies were then compared to those computed using the published formulas. To verify the findings, a series of parametric studies on pile groups embedded in stratified soil was performed where the parameters of the soils were derived based on a back analysis on a case study of a single pile axial loading test in South Jakarta. The results show that the axial pile group efficiency in cohesive soil would be less than or equal to one, whereas in cohesionless soil would be more than or equal to one, especially at pile spacing more than three times the pile diameter. Meanwhile, similar results as found in cohesionless soil were obtained for the stratified soil case.

1 Introduction

Pile foundation is essential to many large civil structures such as bridges and high-rise buildings. It is used to transmit the loads from the upper structures to deeper soil layers that typically have higher soil-bearing capacity. This makes pile foundations have a larger axial and lateral bearing capacity compared to shallow foundations such as strip and spread footings. Still, because the loads are typically larger than the individual pile-bearing capacities, pile foundations are commonly constructed in a group where several piles are placed with a minimum spacing from one pile to another of 2.5 times the pile diameter [1]. This is later called a pile group.

In a pile group, the pile heads are connected to the pile cap to distribute the loads from the upper structures to the piles. This arrangement can further increase the overall load-carrying capacity of a pile group. However, as noted in [2-4], the ultimate capacity of a vertically loaded pile group is not certainly the sum of the individual pile's capacities within the group. The difference in the bearing capacity value is due to the overlapping stress zone produced by each pile within the group [3-4]. This phenomenon is later called the group effect and is expressed through the group efficiency factor (E_g) which is defined as the ratio between pile group capacity to the summation of the individual piles capacity in a group [5].

Many empirical formulas for estimating the E_g value have been published and used in various projects such as Sayed & Bakeer [5], Converse-Labarre [6], Seiler-Keeney [7], Feld [8], Los Angeles Group Action [9], and Ferchat's [10] formulas. Most of the formulas only consider the number of piles, pile spacing, pile configuration, and/or pile dimension, and do not take into account the pile or soil conditions [5, 10]. For instance, the E_g value of Feld's formula [8] is only a function of the number of piles. According to Feld's formula, the capacity of an individual pile within a pile group reduces by $^1/_{16}$ because other piles are placed in the horizontal, vertical, or diagonal directions, regardless of the pile diameter, pile spacing, and soil type. In contrast, previous studies [5, 10-12] found that soil conditions and pile spacing affected the E_g value.

Several studies on the E_g value have indicated that the group efficiencies in cohesive and cohesionless soils are different. Researchers in [13] reported on five pile group load tests in clay, all of which yielded E_g values close to unity. Similar findings were also presented in [14] that the E_g values of model tests on pile groups embedded in clay were always less than one. Meanwhile, researchers in [10] investigated the efficiency of some pile group configurations embedded in soft clays by using a numerical approach, FLAC3D, and found the efficiencies were often less than unity. Thus, applying $E_g > 1$ could lead to an overestimated bearing capacity of a pile group embedded in clay [10].

*Corresponding author: widjaja@unpar.ac.id

Meanwhile, for group piles in cohesionless soils, the E_g value exceeded 1 for the six full-scale pile group load tests in sands [13]. Then, according to the reference in [16], the efficiency of the axially loaded pile groups installed in densely compacted sand was larger than one. The ASCE Committee on Deep Foundations report [15] also suggested group efficiency for friction piles in cohesionless soils at the spacing between 2 to 3 times the pile diameters was larger than or equal to unity. The reasons for $E_g > 1$ in cohesionless soils were mainly due to pile displacement and driving vibrations which increased the density of the cohesionless soil in the vicinity of the pile. The soil densification was further continued as the other piles were driven or installed nearby [3]. However, in a situation where the cohesionless soil is in a very loose-to-loose state with a high groundwater level, the E_g value could be less than one [11].

Furthermore, another issue is that each pile group efficiency formula produces a different E_g value and it is typically less than one. For instance, consider a square pile group configuration of 2 × 2 (4 piles) where each pile diameter is 0.8 m and the pile spacing (S_p) is 2.4 m or three (3) times the diameter (D). The Converse-Labarre [6], Seiler-Keeney [7], Feld [8], and Los Angeles Group Action [9] formulas produce an E_g value of 0.80, 0.94, 0.81, and 0.86, respectively. Although the values do not vary widely, the value discrepancy can result in an overestimated or underestimated magnitude of the pile group's ultimate bearing capacity ($Q_{g,gp}$).

According to the aforementioned issues, this paper aims to study the effects of the number of piles in a pile group and soil type on the E_g and load-carrying behaviors of pile groups embedded in cohesive and cohesionless soils, and also in the stratified soil condition using the three-dimensional (3D) finite element analysis. It is worth noting that the finite element method was used in this study due to its advantages to model complex cases and soil behavior. The 3D finite element simulations were carried out to obtain the load-settlement of single pile and pile groups. Later, load-settlement responses were interpreted using Davisson's method [17] and Chin's method [18] to obtain the ultimate bearing capacity of the single pile and the pile groups. Eventually, the E_g value was obtained by dividing the ultimate bearing capacity of the single pile by the pile group's ultimate bearing capacity and then comparing it to those computed using the empirical E_g formulas.

2 Pile group efficiency formulas

Several pile group efficiency formulas have been developed and some of the most commonly used pile group efficiency formulas in practices are Converse-Labarre [6], Seiler-Keeney [7], Feld's [8], Los Angeles Group Action [9], and simplified formula [9] methods.

2.1 Converse-Labarre method

According to the Converse-Labarre method [6], pile group efficiency (E_g) is a function of the number of piles in a pile group, pile diameter (D), and pile spacing (S_p). Equation 1 shows the Converse-Labarre equation:

$$E_g = 1 - \left[\frac{(n_1 - 1)n_2 + (n_2 - 1)n_1}{90 n_1 n_2}\right]\theta \tag{1}$$

where θ is $\tan^{-1}(D/S_p)$, n_1 is the number of columns in a pile group, and n_2 is the number of rows in a pile group.

2.2 Seiler-Keeney method

Seiler-Keeney method [7] defines the E_g formula as shown in Equation 2.

$$E_g = \left[1 - \frac{36 S_p (n_1 + n_2 - 2)}{(75 {S_P}^2 - 7)(n_1 + n_2 - 1)}\right] + \frac{0.3}{n_1 + n_2} \tag{2}$$

2.3 Los angeles group action method

Equation 3 shows the Los Angeles Group Action method [9] to estimate the E_g value:

$$E_g = 1 - \frac{D}{\pi S_P n_1 n_2}\left[n_1(n_2 - 1) + n_2(n_1 - 1) + (n_2 - 1)(n_1 - 1)\sqrt{2}\right] \tag{3}$$

2.4 Simplified formula

Simplified Formula [9] expresses the E_g formula as shown in Equation 4.

$$E_g = \frac{2(n_1 + n_2 - 2)S_p + 4D}{p n_1 n_2} \tag{4}$$

where p is the perimeter of the pile.

2.5 Feld's method

Feld method [8] suggested that the individual pile-bearing capacity in a pile group decreased by $^1/_{16}$ due to pile interaction(s) in the horizontal, vertical, or diagonal direction. Fig. 1 illustrates the interactions between piles in 1 × 2, 3, 2 × 2, and 3 × 3 group piles. For instance, the E_g value for a 3 × 3 group pile is $(4 \times {}^{13}/_{16} + 4 \times {}^{11}/_{16} + {}^{8}/_{16})/9 = 0.722$, while for a 2 × 2 group pile is $(4 \times {}^{13}/_{16})/4 = 0.813$.

3 Case study and numerical analysis

3.1 Case study

This paper used a case study of a 35-floors apartment in Fatmawati, South Jakarta. The apartment was designed to have one ground floor, one floor of semi-basement, and 3 floors of the basement. Thus, the foundation cut-off level was located at 15 m below the existing ground level (GL -15 m). Bored piles with D = 1.2 m and 17 m in length (L) measured from the cut-off level were used as the foundation of the apartment.

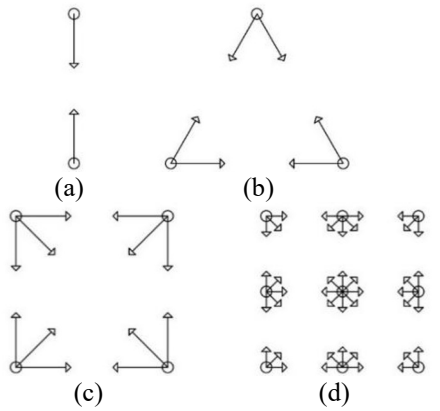

Fig. 1. Piles interactions in a (a) 1 × 2, (b) 3, (c) 2 × 2, dan (d) 3 × 3 pile groups.

The soil investigation in this case study consisted of eleven (11) Standard Penetration Tests (SPT) and one (1) Cone Penetration Test (CPT). Fig. 2 shows one of the N_{SPT} profiles against elevation used in this study and the soil stratification at the site. Note that the used SPT shown in Fig. 2 was conducted at an elevation of -4 m (GL -4.0 m) below the ground surface (GL ±0.0 m). The SPT test results show that the soil profile is dominated by medium to hard silt and very dense, denoted by V. Dense, sand soil layers. Similar soil profiles were also found in other boreholes. In addition, the groundwater level at the site was located around GL -5.2 m to -8.7 m.

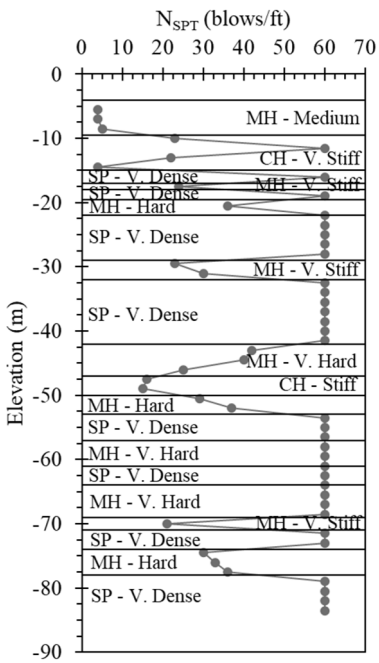

Fig. 2. N_{SPT} vs. elevation.

3.2 Numerical analyses and parametric studies

A three-dimensional finite element program was used in this study to model the group piles. The Mohr-Coulomb material model (MC-Model) was adopted in this research to model the stress-strain response of the cohesive and cohesionless soils. The MC-Model requires several basic, strength, and stiffness input parameters, such as the soil natural unit weight (γ), saturated unit weight (γ_{sat}), undrained shear strength (s_u), effective cohesion (c'), effective friction angle (ϕ'), effective Poisson's ratio (υ'), and effective Young's modulus (E'). Those parameters were obtained from the laboratory test results and empirical correlations with N_{SPT} value or physical soil properties from various researchers.

The ϕ' value for cohesionless soils was determined using Wolff's empirical correlation [19]. Meanwhile, for cohesive soils, the ϕ' value was determined using Sorensen and Okkels's correlation [20]. The s_u value was estimated using Terzaghi & Peck's [21] and Sower's [22] empirical correlations with N_{SPT}. Referring to Das's [9] empirical correlation between υ' and soil type and consistency, $\upsilon' = 0.3$ was assumed for very dense sand, very stiff or hard clay, and medium silt. Meanwhile, for very stiff or very hard silt, $\upsilon' = 0.25$ was taken. Then, the E' value for cohesionless soil was estimated to be equal to 4000 N_{SPT} [23]. According to [3], the undrained Young's modulus (E_u) and E' of cohesive soil were respectively equal to $1175s_u$ and $E' = 80\%E_u$.

Jaky's [24] and Kulhawy and Mayne's [25] semi-empirical correlations were adopted to estimate the coefficient of lateral earth pressure at rest for overly consolidated cohesive soil (K_0^{OC}) based on the ϕ' value and over consolidation ratio (OCR). Meanwhile, for cohesionless soil, the coefficient of lateral earth pressure at rest (K_0) was estimated using the same approach as K_0^{OC} with OCR = 1. Then, the soil-pile interfaces were modeled on the pile surface and at the pile tip with an interface reduction factor (R_{inter}) equaled to 1 or rigid.

Furthermore, the linear elastic material model was adopted to model the stress-strain relationship of the piles and the pile cap. The piles had D = 1.2 m and an effective length (L_{eff}) of 17 m (i.e., the effective length was the embedded length of the pile in soil). The pile cap was situated at 1 m above the ground surface to avoid influences of the pile cap on the pile group bearing capacity. Prescribed displacement was then applied on the pile head for the single pile and on the pile cap for the pile group in the loading phases to model the pile settlement at the pile head. Note that the pile cap in this study was designed to be rigid so that the pile group's vertical displacement would be relatively uniform.

The finite element model boundaries were set to 25D measured from the pile center for the x- and y-axis and $3L_{eff}$ at minimum measured from the bottom of the pile for the z-axis to minimize the boundary effect. Fig. 3 shows the model boundaries for the single pile model and soil stratification in the numerical analysis. The general setting of the mesh was medium. However, some mesh adjustments were necessary to avoid numerical errors during computation.

The estimated soil parameters in this study were later back-analyzed to match the modeled stress-strain response of the soils in the numerical analysis to the measured field response. A full-scale axial pile loading test was then simulated in the finite element program to obtain the load-settlement curve which was later compared to that obtained from the field measurement. It was worth noting that in this paper, the back analysis was focused on the soil-pile responses to axial

compressive load. Then, in the numerical simulation, the excavation to GL -15 m was also simulated and the groundwater level was situated at GL -6.95 m in accordance with the boring and SPT tests. The results of the back analysis are shown in Table 1 for the calibrated soil parameters and in Fig. 4 for the load-settlement curves. The continuous line in Fig. 4 represents the load-settlement curve obtained from field measurement, whereas the dashed line is the load-settlement curve based on the back analysis.

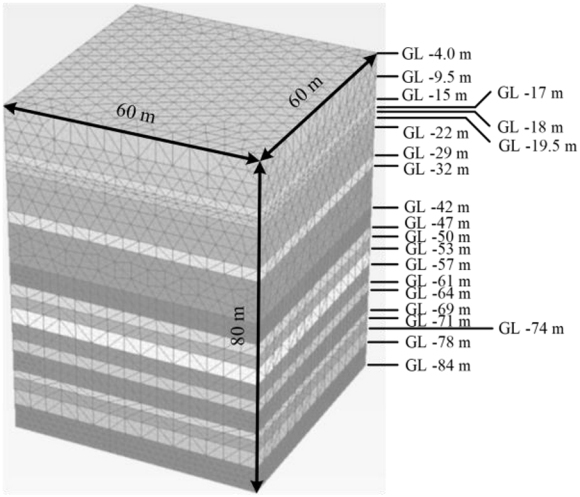

Fig. 3. Finite element model.

Table 1. Calibrated soil parameters.

Elevation (m)	γ (kN/m^3)	γ_{sat} (kN/m^3)	s_u (kN/m^2)	ϕ' (°)	E' (kN/m^2)	K_0^{OC}
4 – 9.5	15.5	16.0	40	-	37,600	0.84
9.5 – 15	15.5	16.0	300	-	282,000	0.86
15 – 17	15.5	16.0	-	43	240,000	0.32
17 – 18	15.5	16.0	240	-	225,600	0.84
18 – 19.5	15.5	16.0	-	43	240,000	0.32
19.5 – 22	15.5	16.0	360	-	338,400	0.84
22 – 29	15.5	16.0	-	43	240,000	0.32
29 – 32	18.0	18.3	300	-	282,000	0.84
32 – 42	18.0	18.3	-	43	240,000	0.32
42 – 47	18.0	18.3	400	-	376,000	0.85
47 – 50	18.0	18.3	160	-	150,400	0.86
50 – 53	16.2	16.8	350	-	329,000	0.85
53 – 57	16.2	16.8	-	43	240,000	0.32
57 – 61	16.2	16.8	600	-	564,000	0.75
61 – 64	16.2	16.8	-	43	240,000	0.32
64 – 69	16.2	16.8	600	-	564,000	0.75
69 – 71	16.2	16.8	210	-	197,400	0.75
71 – 74	16.2	16.8	-	43	240,000	0.32
74 – 78	16.2	16.8	350	-	329,000	0.75
78 – 84	16.2	16.8	-	43	240,000	0.32

Numerical parametric studies were also performed in this study to investigate the effects of the number of piles on the E_g value and the load-carrying behavior of pile groups in different soil types. In the parametric study, the pile groups were embedded in a homogeneous medium clay and very dense sand, and also in the stratified soil layer based on the case study presented in this paper. Table 2 shows the soil parameters used for the homogenous cohesive and cohesionless soils. The parameters in Table 2 were selected from the calibrated soil parameters in Table 1. Note that, for analyses in homogenous soil conditions, no excavation and dewatering were modeled and the groundwater level was at the ground surface. Furthermore, the pile group configurations were set to 2 × 2, 3 × 3, 4 × 4, 5 × 5, and 6 × 6 with pile spacing of 2D, 3D, and 4D for each configuration.

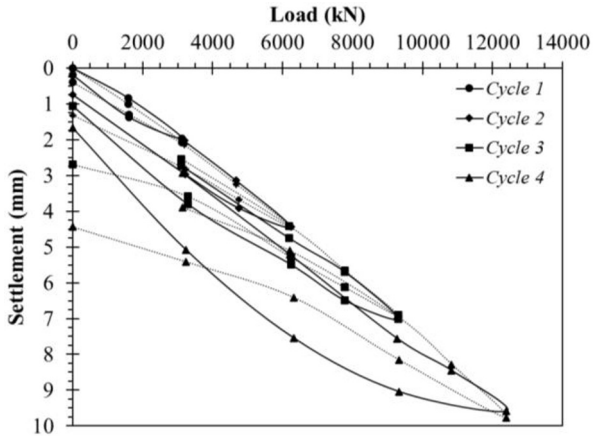

Fig. 4. Load settlement curves.

Table 2. Homogeneous soil parameters.

Soil Type	γ (kN/m^3)	γ_{sat} (kN/m^3)	s_u (kN/m^2)	ϕ' (°)	E' (kN/m^2)	K_0^{OC}
Medium Clay	15.5	16.0	40	-	37,600	0.84
Very Dense Sand	18.0	18.3	-	43	240,000	0.32

Finally, the ultimate bearing capacities of single ($Q_{g,s}$) and group piles ($Q_{g,gp}$) were estimated from the load settlement curve obtained from the numerical analysis using Chin's method (1970) and Davisson's method (1972). Then, the pile group efficiencies were computed by dividing the $Q_{g,gp}$ by the sum of the single pile's ultimate bearing capacity in the pile group ($\Sigma Q_{g,s}$). The numerical-based pile group efficiency was then compared to several published formulas.

4 Results and discussions

4.1 Pile group efficiencies in cohesive soil

Fig. 5 shows the E_g values for various pile spacing and number of piles installed in a homogeneous cohesive soil. The results in Fig. 5 indicate that the E_g values for pile spacings 2D, 3D, and 4D and pile configurations 2 × 2, 3 × 3, 4 × 4, 5 × 5, and 6 × 6 were generally less than unity indicating that the $Q_{g,gp}$ was smaller than the total $Q_{g,s}$ in the pile group. This was attributed to the overlapping stress zone within the pile group [10]. Moreover, the E_g values obtained from the numerical analyses in this study, or so-called numerical E_g, were decreasing with increasing the number of piles and decreasing the pile spacing. The numerical E_g's were generally less than one and also relatively smaller than those obtained from the empirical formulas, especially

for the pile groups with a 2 × 2 pile configuration. Meanwhile, for the 3 × 3 and 4 × 4 pile groups, the E_g's were close to those computed using Converse-Labarre's formula. These findings applied to the all of E_g values where the $Q_{g,s}$ and $Q_{g,gp}$ values were interpreted using Davisson's method [17] and Chin's method [18]. This implies that the empirical formula-based E_g resulted in a relatively underestimated or overestimated E_g value of a pile group in cohesive soil.

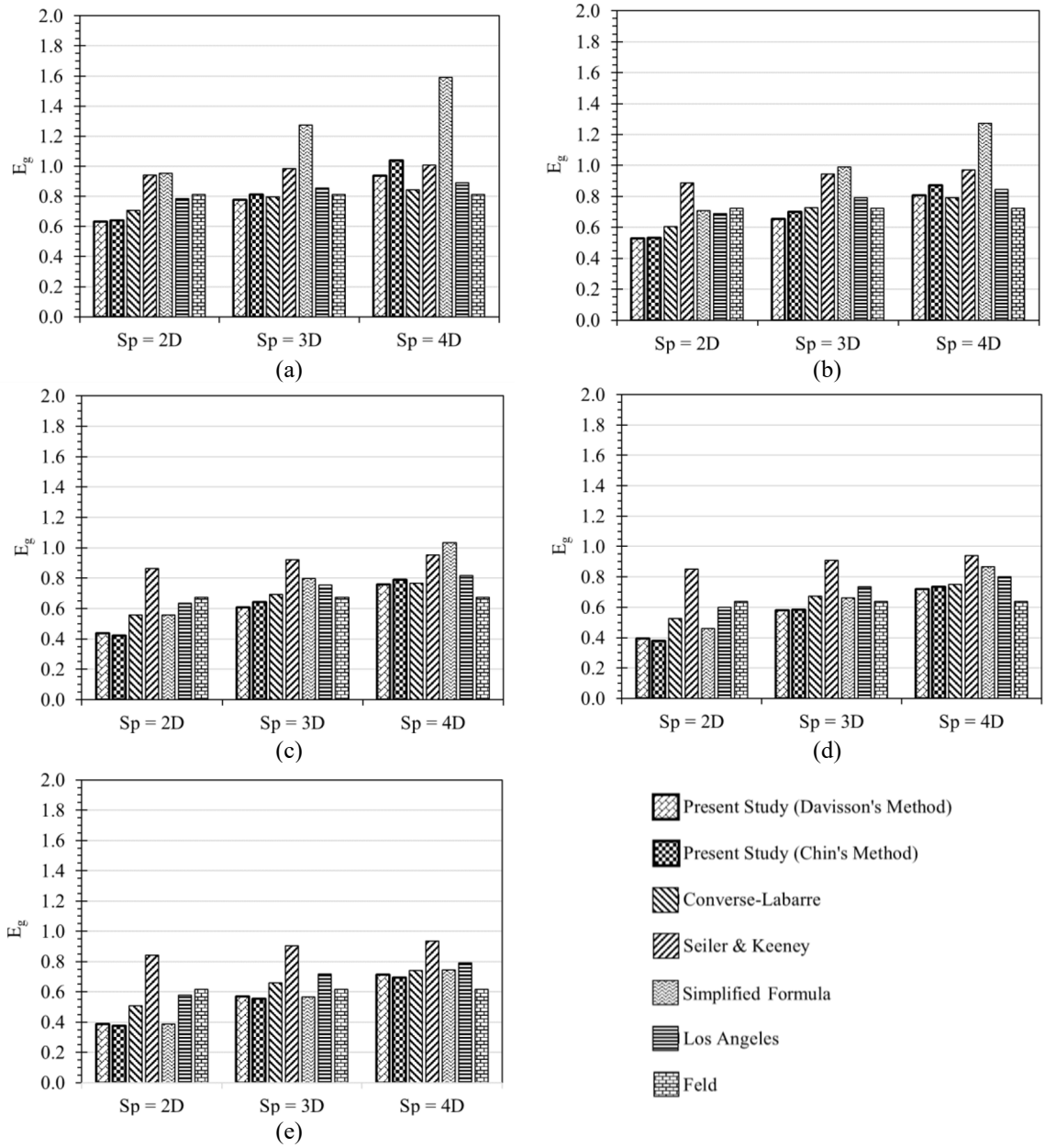

Fig. 5. Pile group efficiencies in cohesive soil obtained from the finite element analyses and several published formulas for pile groups (a) 2 × 2, (b) 3 × 3, (c) 4 × 4, (d) 5 × 5, and (e) 6 × 6.

It was worth noting that not all of the empirical formulas could capture the effects of pile spacing on the E_g value. For instance, the E_g values obtained from Feld's method remained constant, although the S_p value was increased. This signified Feld's method could not capture the effect of pile spacing. However, Feld's method resulted in comparatively close E_g values to the numerical E_g for S_p > 2D. Then, the simplified formula also resulted in an unrealistically large E_g's (i.e., E_g > 1) for a relatively small number of piles (i.e., 2 × 2), whilst other approaches predicted E_g < 1. However, in this case, the simplified formula produced a quite similar E_g value to the numerical E_g for pile group configuration 6 × 6. Then, the E_g values produced by using Seiler & Keeney's formula were generally higher than the numerical E_g.

To further understand the pile group's load-carrying and failure mechanisms in cohesive soils, the distribution of the mobilized shear strength (τ_{mob}) around the pile was studied. Note that as the undrained effective stress analysis with undrained shear strength and effective stiffness parameters was adopted in this study, the maximum shear stress (τ_{max}) in this study was equal to s_u and it was not affected by the stress changes in the soil. Fig. 6 displays the τ_{mob} contours for the 6 × 6 group pile embedded in cohesive soil with S_p = 2D, 3D, and 4D at the same vertical displacement, 80 mm. In Fig. 6, the warmer the color (i.e., red color) indicates the

higher the magnitude of the $\tau_{mob,}$ and the τ_{mob} ranges from 0 to 56 kN/m^2.

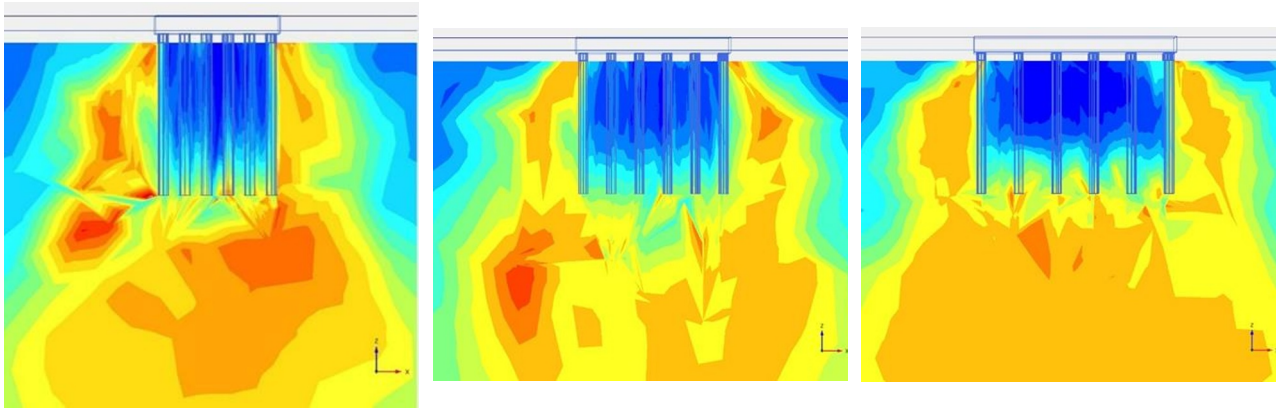

(a) (b) ©

Fig. 6. Contours of τ_{mob} in the homogeneous cohesive soil case for pile group with (a) S_p = 2D, (b) S_p = 3D, and (c) S_p = 4D at 80 mm vertical displacement.

As shown in Fig. 6, in cohesive soil, the τ_{mob} along the pile group's perimeter and at the tip of the pile group was relatively large compared to the τ_{mob} value between the piles. This indicates the piles and soil in between the piles in the pile groups in cohesive soil worked together behaving as a block in distributing the working load to the perimeter of the pile group and at the tip. The movements of piles and soil in between the piles were also relatively uniform resulting in a low τ_{mob} value, represented by the dark and light blue colors in Fig. 6. At this condition, the friction and tip resistances of the block of piles controlled the $Q_{g,gp}$. Then, increasing the pile spacing in the pile group increased the block dimension and resulted in a wider area of τ_{mob} and higher $Q_{g,gp}$. This behavior was also observed for the pile group with S_p = 2D, 3D, and 4D.

4.2 Pile group efficiencies in cohesionless soil

In contrast to the results for pile groups in cohesive soil, the numerical E_g values for pile groups in cohesionless soil were greater than one (1). This signifies that the $Q_{g,gp}$ was greater than the sum of the $Q_{g,s}$ times the number of piles in the pile groups. Fig. 7 shows the E_g values for various pile spacing and the number of piles in the pile groups installed in the homogeneous cohesionless soil. However, it was a common trend that increasing the pile spacing in the pile group increased the magnitude of E_g for the same pile configuration. It was also found that the E_g value increased with increasing the number of piles in the pile groups and became relatively constant when the number of piles was greater than 3 × 3. Similar results were presented in previous research conducted in [16] and [26].

Note that the E_g values computed by using the empirical formulas for the pile group in cohesionless soil were the same as those obtained for the pile group in cohesive soil (Fig. 5). Then, as depicted in Fig. 7, the empirical formula-based E_g values were also generally smaller than the numerical E_g. Those signified that the empirical formulas were independent of soil type and also underestimated the magnitude of E_g for pile groups in cohesionless soil. In fact, soil type affected the E_g value.

The distribution of τ_{mob} around the pile groups embedded in cohesionless was also investigated in this section. Note first that the τ_{max} for cohesionless soil in this study is computed as $0.5(\sigma'_1 + \sigma'_3)\sin\phi' + c'\cos\phi'$ where σ'_1 is the largest compressive (or smallest tension) principal stress, σ'_3 is the smallest compressive (or largest tension) principal stress, ϕ' is the effective friction angle, and c' is the effective cohesion and equal to nil. This equation implies that the magnitude of τ_{max} changes with the change of the principal stresses. Higher principal stresses yield a higher τ_{max} value.

Fig. 8 exhibits the τ_{mob} contours for pile groups in cohesionless soil with S_p = 2D, 3D, and 4D at 80 mm vertical displacement. As depicted in Fig. 8, high τ_{mob} value, represented by the red and orange colors, tended to accumulate around the tip of the pile group. Similar to the τ_{mob} contours for pile groups in cohesive soil, the τ_{mob} in soil in between the piles in the pile groups was also relatively low compared to the surrounding τ_{mob}, especially at the tip of the pile group. This indicates that there was densification at the tip of the pile groups due to compressive load resulting in a higher shear strength around the tip and higher $Q_{g,gp}$ of the pile groups compared to the sum of $Q_{g,s}$ times the number of piles in the pile groups.

4.3 Pile group efficiencies in case study

To verify the results obtained for homogeneous soil conditions, a similar parametric study on the effects of the number of piles in the pile group and pile spacings on E_g values were carried out in the stratified soil condition based on the described case study in this paper. Fig. 9 shows the E_g values for pile groups with various numbers of piles and S_p's in the stratified soil condition. The E_g value increased with increasing S_p for the same pile configurations and reached $E_g > 1$ when $S_p > 3D$. A relatively high E_g value (i.e., $E_g \geq 1$) could be attributed to the cohesionless soil dominance in the site. Then, it was found that the E_g value in stratified soil conditions was not necessarily increasing or decreasing

with the increase in the number of piles in the pile group. However, it was clear in Fig. 9 that the E_g values still increased with increasing pile spacing. Furthermore, the magnitudes of the empirical formula-based E_g's remained the same as those computed for the pile groups in cohesive and cohesionless soils. This implies that soil type (i.e., cohesive or cohesionless soil) greatly affected the E_g value and the empirical formula-based E_g's could not capture different responses of group piles embedded in cohesive or cohesionless soils. Finally, the published empirical formulas produced an overestimated or underestimated E_g.

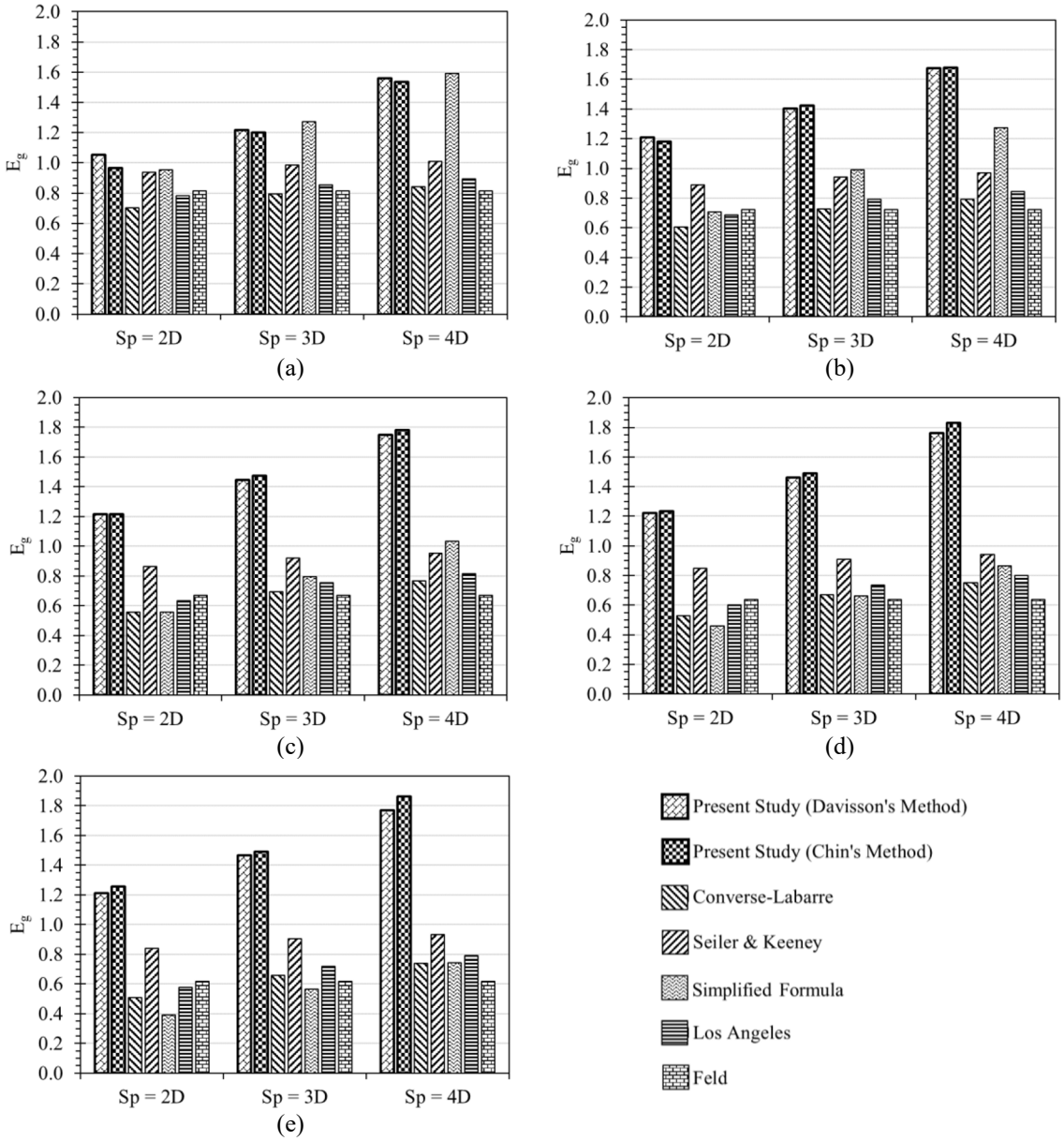

Fig. 7. Pile group efficiencies in cohesionless soil obtained from the finite element analyses and several published formulas for pile groups (a) 2 × 2, (b) 3 × 3, (c) 4 × 4, (d) 5 × 5, and (e) 6 × 6.

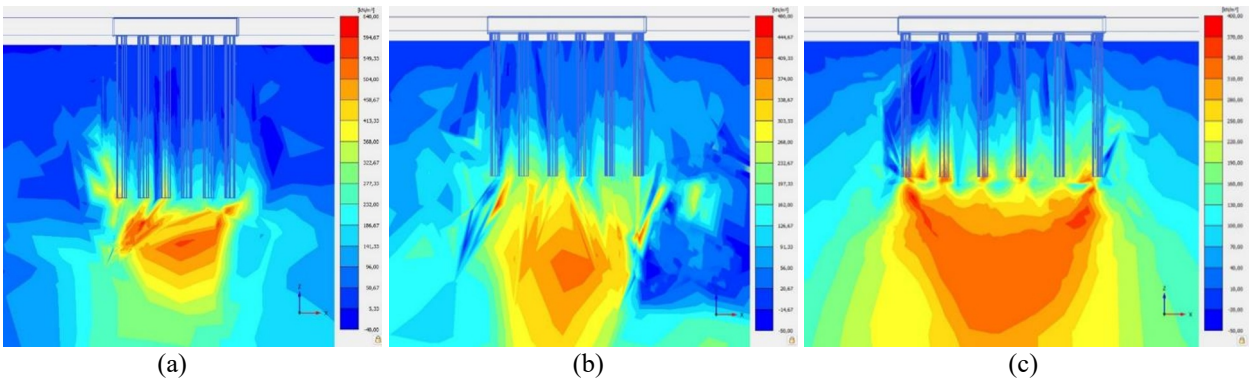

Fig. 8. Contours of τ_{mob} in the homogeneous cohesionless soil case for pile group with (a) S_p = 2D, (b) S_p = 3D, and (c) S_p = 4D at 80 mm vertical displacement.

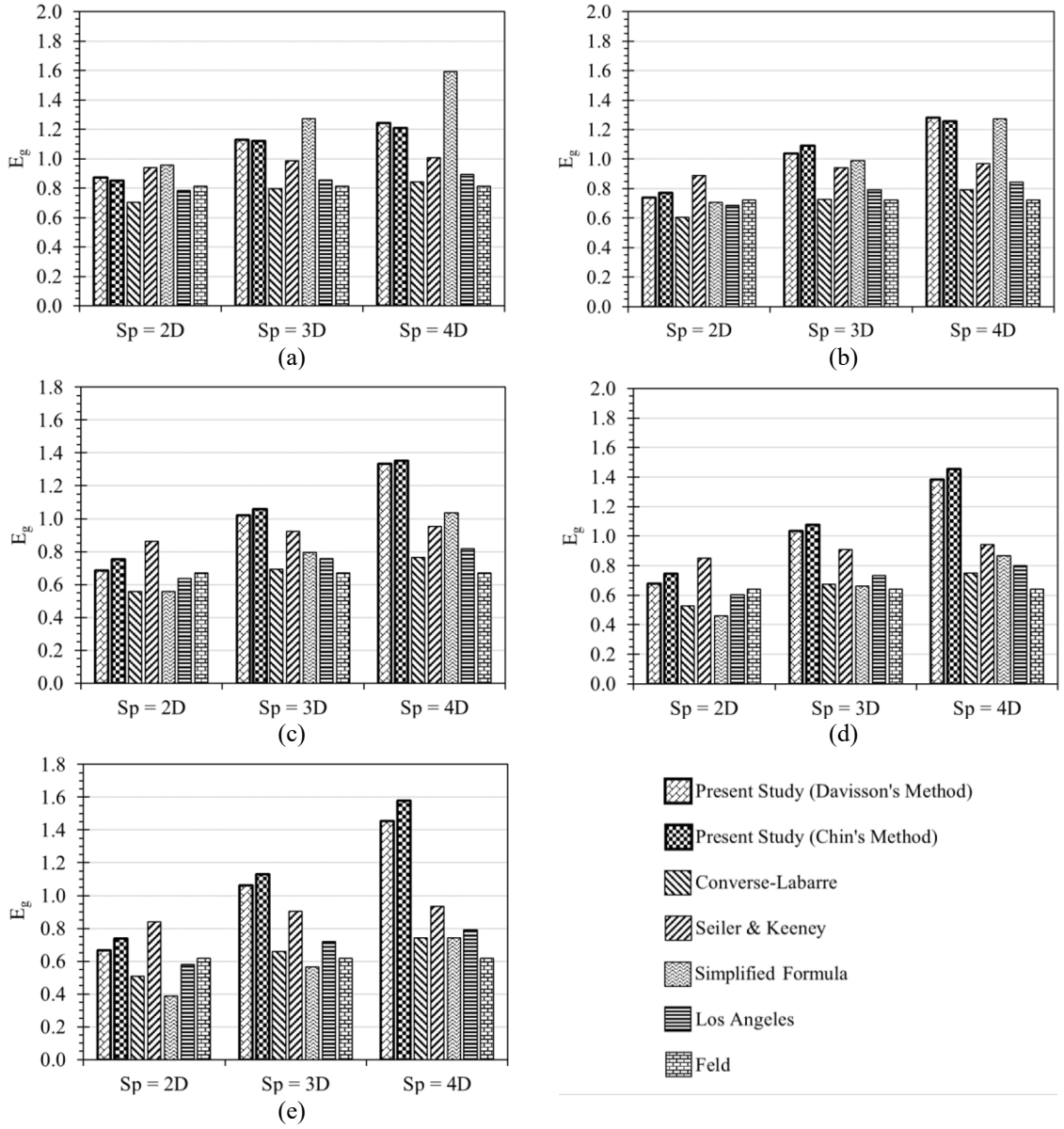

Fig. 9. Pile group efficiencies in stratified soil condition obtained from the finite element analyses and several published formulas for pile groups (a) 2 × 2, (b) 3 × 3, (c) 4 × 4, (d) 5 × 5, and (e) 6 × 6.

5 Conclusions

This paper studied the effects of the number of piles and pile spacing in a pile group embedded in cohesive, cohesionless, and stratified soil conditions on the pile group efficiency and behavior in carrying axial compressive load using a three-dimensional finite element approach. The findings of this study could then be summarized as follows:

(1) In cohesive soil, the greater the number of piles in a pile group and the smaller the pile spacing, the smaller the pile group efficiency;

(2) The pile group efficiency in cohesive soil was generally less than one, except for 2 × 2 and 3 × 3 pile configurations with pile spacing greater than or equal to three times the pile diameter, although the pile spacing was greater than three times the pile diameter, and the magnitudes were lower than those estimated using the published pile group efficiency formulas;

(3) According to the mobilized shear strength contours in the homogeneous cohesive soil, it was indicated that the pile group behaved as a block distributing shear stresses to the perimeter and at the tip of the pile group;

(4) Increasing the number of piles and pile spacing in a pile group in cohesionless soil increased the pile group efficiency;

(5) The numerical pile group efficiency of the pile groups in cohesionless soil was generally greater than or equal to one. This was due to sand densification, especially at the tip of the pile groups indicated by the large mobilized shear strength value. Thus, it was suggested to use pile group efficiency equaled one for pile groups embedded in cohesionless soils;

(6) The axial pile group efficiencies in stratified soil conditions were higher than pile group efficiency in cohesive soil, but it is still smaller than the value of pile group efficiency in cohesionless soil. This was mainly because the soil layers at the site were dominated by cohesionless soil with thin layers of cohesive soil;

(7) The change of the pile group efficiency with pile spacing in the stratified soil condition was relatively similar to those obtained for pile groups in homogeneous cohesive and cohesionless soils. It increased with increasing pile spacing. However, the pile group efficiencies did not always increase or decrease with an increasing number of piles. The group effect diminished as the pile spacing increased, and increased the ultimate bearing capacity of the pile group.

(8) The published pile group efficiency formulas were over- or underestimated the pile group efficiency in cohesive, cohesionless, and stratified soil conditions. This was because the published pile group efficiency formulas did not consider different soil stress-strain behavior and stress distributions under axial compressive load from a pile group. However, it was conservative to adopt the published formulas for estimating the pile group efficiency in cohesionless soils, but not in cohesive soil.

References

1. National Standardization Agency, Geotechnical Design Requirements (SNI 8460:2017)
2. J.S. Pressley, H.G. Poulos, International Journal for Numerical and Analytical Methods in Geomechanics **10**(2), 213-221 (1986) https://doi.org/10.1002/nag.1610100208
3. J.E. Bowles, Foundation analysis and design 5th Ed. (1988)
4. M. Tomlinson, J. Woodward, Pile design and construction Practice, 5th ed. (The McGraw-Hill Companies, Inc., 2008)
5. S.M. Sayed, R.M. Bakeer, Journal of Geotechnical Engineering **118**(2), 278-299 (1992) https://doi.org/10.1061/(ASCE)0733-9410(1992)118:2(278)
6. H.W. Bolin, Building Standards Monthly **10**(1), 4-5 (1941)
7. J.F. Seiler, W.D. Kenney, Wood Preserving News **22**(11), 109-118 (1944)
8. J. Feld, Trans. ASCE **108** (1943)
9. B.M. Das, N. Sivakugan, Principles of foundation engineering 8th Ed. (Cengage Learning, 2015)
10. A. Ferchat, M.N. Houhou, S. Benmebarek, World Journal of Engineering **18**(3), 397-406 (2021) https://doi.org/10.1108/WJE-04-2020-0112
11. N.F. Ismael, Journal of Geotechnical and Geoenvironmental Engineering **127**(9), 766-773 (2001) https://doi.org/10.1061/(ASCE)1090-0241(2001)127:9(766)
12. P.A. Tuan, Int. J. Sci. Eng. Res. **7,** 7 (2006)
13. A.S. Vesic, Design of pile foundations (National Cooperative Highway Research Program, 1977)
14. M.W. O'Neill, *Group action in offshore piles*, in Proceedings of the Conference on Geotechnical Practice in Offshore Engineering, 27-29 April 1983, Austin Texas (1983)
15. American Society of Civil Engineers Committee on Deep Foundations, Practice guideline for the selection, design, and installation piles (American Society of Civil Engineers, 1984)
16. M.K. Elsamny, M.A. Ibrahim, S.A. Gad, M.F. Abdel-Mageed, Int. J. Eng. Res. Technol **6**, 5 (2017)
17. M.T. Davisson, *High capacity piles*, in Proceedings of the Lecture Series: Innovations in Foundation Construction, 22 March 1972, Chicago (1972)
18. F.K. Chin, *Estimation of the ultimate load of piles from tests not carried to failure*, in Proceedings of the 2nd Southeast Asian Conference on Soil Engineering, 11-15 June 1970, Singapore (1970)
19. T.F. Wolff, *Pile capacity prediction using parameter functions*, in Proceedings of Predicted and Observed Axial Behavior of Piles: Results of a Pile Prediction Symposium (Geotechnical Special Publication No. 23), 25 June 1989, Illinois (1989)
20. K.K. Sorensen, N. Okkels, *Correlation between drained shear strength and plasticity index of undisturbed overconsolidated clays*, in Proceedings of the 18th International Conference on Soil Mechanics and Geotechnical Engineering, 2-6 September 2013, Paris (2013)
21. K. Terzaghi, R. Peck, Soil mechanics in engineering practice 2nd Ed. (New York John Wiley & Sons, 1967)
22. G.F. Sowers, Introductory soil mechanics and foundations 4th Ed. (Pearson College Div, 1979)
23. M. Khoiri, C.Y. Ou, Computers and Geotechnics **47**, 57-67 (2013) https://doi.org/10.1016/j.compgeo.2012.06.009
24. J. Jaky, *Pressure in silos*, In Proceedings of the 2nd International Conference on Soil Mechanics and Foundation Engineering, 21–30 June 1948, Rotterdam (1948)
25. P.W. Mayne, F.H. Kulhawy, Journal of the Geotechnical Engineering Division **108**(6) (1982) https://doi.org/10.1061/AJGEB6.0001306
26. E. Nasrollahzadeh, N. Hataf, International Journal of Geotechnical Engineering **16**(4), 426-437 (2022) https://doi.org/10.1080/19386362.2019.1651042